PEDIATRIC IMAGING

I J Radiol. 2024 October; 21(4): e158779 https://doi.org/10.5812/iranjradiol-158779

Published Online: 2024 October 31 **Research Article**

Comparative Effects of Model-Based and Adaptive Statistical Iterative Reconstruction Algorithms on Image Quality Metrics in Low-Dose Chest Computed Tomography for Pediatric Pneumonia: A Prospective Study

Yizhai Ye [1], Ruirui Chen [2], Weigen Wang [1], Jianhua He [1], Minggai Ge [3], Sifang Zhou [4,*]

[1] Department of Radiology, Ninghai First Hospital, Ningbo 315600, Zhejiang Province, China
[2] Baiyang Community Health Service Center (Baiyang Women and Children's Health Service Station), Hangzhou 310000, Zhejiang Province, China
[3] Department of Dermatology, No. 908 Hospital of the PLA Joint Logistics Support Force, Nanchang 330001, Jiangxi Province, China
[4] Department of Pediatrics, Nanchang People's Hospital, Nanchang 330001, Jiangxi Province, China

[*] ***Corresponding Author:*** Nanchang People's Hospital, Nanchang 330001, Jiangxi Province, China. Email: zhousfnph@ph-edu.cn

Received: 10 June, 2024; **Revised:** 25 October, 2024; **Accepted:** 28 October, 2024

Abstract

Background: Pneumonia is a common respiratory disease in children, frequently requiring imaging for diagnosis and treatment evaluation. Optimizing image quality is crucial to ensure diagnostic accuracy while minimizing radiation exposure. Comparing advanced image reconstruction algorithms can help achieve this balance.

Objectives: We aimed to compare the effects of the model-based iterative reconstruction (MBIR) algorithm and the adaptive statistical iterative reconstruction (ASIR) algorithm on the noise and overall image quality of low-dose chest computed tomography (CT) for pediatric pneumonia.

Patients and Methods: This was a prospective study. A total of 102 children diagnosed with pneumonia between June 2023 and May 2024 were recruited. All of them underwent a low-dose chest CT scan, and then MBIR and ASIR algorithms were employed for image reconstruction using a simple randomization method (n = 51 in each group). The noise, signal-to-noise ratio (SNR), and contrast-to-noise ratio (CNR) of the reconstructed images were measured and compared. Subjective evaluation of the image quality was performed by two experienced radiologists. The agreement between them was evaluated based on the Kappa value.

Results: The two radiologists provided highly consistent subjective evaluation results for the reconstructed images (Kappa value of 0.85, 95% confidence interval: 0.80 - 0.90). The reconstructed images in the MBIR group were better than those in the ASIR group in terms of image noise, microstructure display, definition of lesion edges, and overall image quality ($P < 0.05$). The dose-length product and effective dose decreased in the MBIR group compared with those in the ASIR group ($P < 0.05$). The SNR and CNR of the lung field, main pulmonary artery, and muscle were higher in the MBIR group than in the ASIR group ($P < 0.05$).

Conclusion: The MBIR algorithm shows more promise than the ASIR algorithm in reducing noise, improving SNR, and maintaining good image quality of low-dose chest CT scans for children with pneumonia, without increasing the radiation dose. Further research may be needed to confirm its broader applicability.

Keywords: Algorithm, Children, Computed Tomography, Image Quality, Pneumonia, Reconstruction

1. Background

Pneumonia is one of the most common respiratory diseases in children. Early and accurate diagnosis, as well as timely and effective treatment, is essential for improving the prognosis of children suffering from pneumonia (1). Among various diagnostic methods, computed tomography (CT) scan is a valuable medical

How to Cite: Ye Y, Chen R, Wang W, He J, Ge M, et al. Comparative Effects of Model-Based and Adaptive Statistical Iterative Reconstruction Algorithms on Image Quality Metrics in Low-Dose Chest Computed Tomography for Pediatric Pneumonia: A Prospective Study. I J Radiol. 2024; 21 (4): e158779. https://doi.org/10.5812/iranjradiol-158779.

imaging examination due to its ability to provide clear and detailed images of lung lesions, enabling accurate assessment of lesion location, size, and morphology (2). However, the high radiation dose is a non-negligible problem faced by conventional CT scans. Such a technique is hazardous to radiation-sensitive groups like children and pregnant women. Exposure to radiation during the critical stages of growth and development may increase the risk of long-term adverse effects, including radiation-induced malignancies (3). This has driven increasing interest in reducing radiation exposure in pediatric imaging while maintaining the diagnostic image quality.

Model-based iterative reconstruction (MBIR) algorithm and adaptive statistical iterative reconstruction (ASIR) algorithm have become new-generation CT image reconstruction techniques in recent years (4). Different from traditional image reconstruction methods, these two algorithms can maintain and even improve image quality while reducing the radiation dose through complicated iterative computation processes (5). The MBIR algorithm achieves repeated iterative optimization of raw data by establishing an accurate physical model with a variety of factors considered, thereby effectively reducing noise and improving the definition and contrast of images. In the ASIR algorithm, prior knowledge and statistical information are utilized to automatically adjust the iterative parameters based on the characteristics of images, generating high-quality images at low doses (6).

Although several studies have evaluated the application of MBIR and ASIR in pediatric chest CT scans, most have focused on general image quality improvements or specific clinical scenarios, such as necrotizing pneumonia (7, 8). However, direct quantitative comparisons of signal-to-noise ratio (SNR) and contrast-to-noise ratio (CNR) across specific anatomical regions (e.g., lung field, pulmonary artery, and muscle) remain limited. Additionally, few studies have comprehensively assessed the potential for dose reduction using these reconstruction techniques for an ultra-low-dose pediatric CT protocol.

2. Objectives

Based on this background, the present study evaluated the effects of the aforementioned two algorithms on optimizing the image quality of low-dose chest CT scans for children with pneumonia, aiming to provide a potentially more precise and safer diagnostic tool. Our findings may have important clinical implications, as they can guide pediatric radiologists in selecting reconstruction algorithms that achieve the lowest possible radiation dose while ensuring diagnostic image quality.

3. Patients and Methods

3.1. Subjects

This was a prospective study. The sample size was determined based on an a priori power analysis conducted using G*Power software. This study was approved by the ethics committee of our hospital, and written informed consent was obtained from the guardians of all enrolled children. A total of 102 children diagnosed with pneumonia in our hospital between June 2023 and May 2024 were enrolled, including 61 boys and 41 girls aged 3.14±2.05 years old. All of them underwent a low-dose chest CT scan, and then MBIR and ASIR algorithms were employed for image reconstruction using a simple randomization method (n = 51 in each group).

The following inclusion criteria were employed: (1) Child patients clinically diagnosed with pneumonia; (2) those examined by low-dose chest CT scan; and (3) those without contraindications to CT scan. The exclusion criteria involved: (1) Child patients complicated with other serious lung diseases; (2) those whose images could not be analyzed due to severely impaired quality; or (3) those who had recently undergone high-dose chest CT scan or other radioactive examinations. The flow chart for subject enrollment is exhibited in Figure 1.

3.2. Computed Tomography Scan Methods

Low-dose CT scanning mode was employed to scan the child patients' chests, with parameters set as follows: Tube voltage at 100 kV, tube current automatically adjusted according to the age and weight of the child, scan slice thickness of 5 mm, and reconstruction interval at 5 mm. All participants in this study were required to complete systematic breathing training prior to scanning, thus ensuring smooth breathing during the scanning process. After scanning, the raw data were saved in the workstation for subsequent processing.

3.3. Image Reconstruction Methods

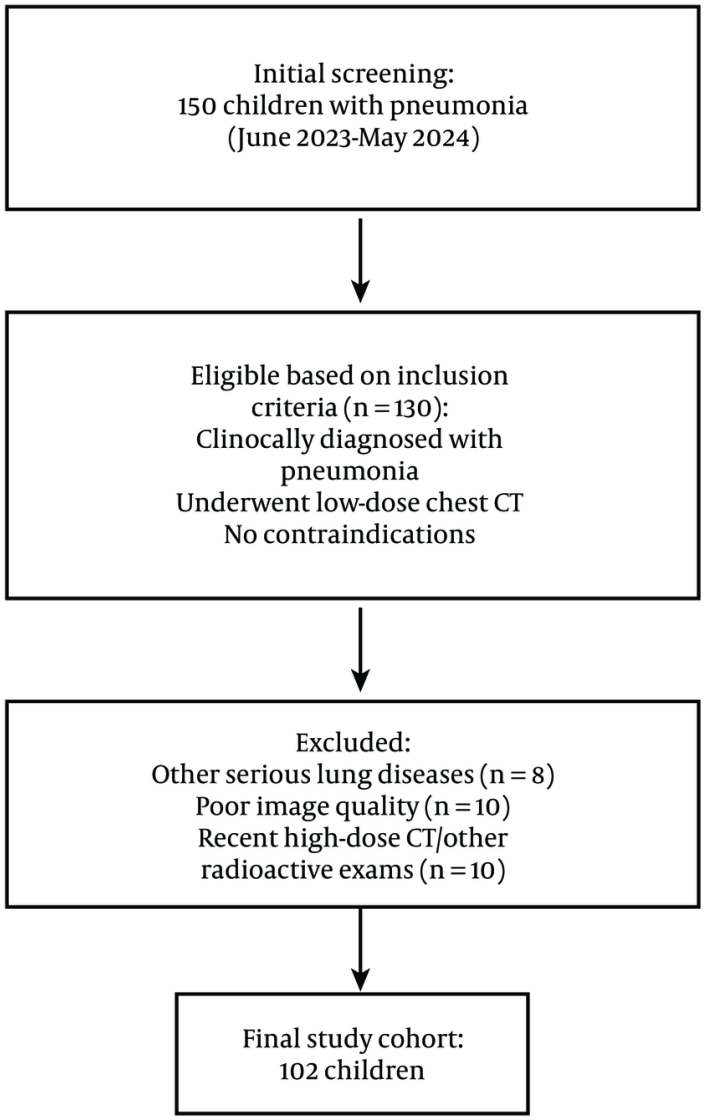

Figure 1. Flow chart for subject enrollment

The raw data were separately reconstructed using the MBIR and ASIR algorithms. In brief, the MBIR algorithm was executed using the specialized software equipped in the GE HD750 scanner, and the ASIR algorithm was performed through the ASIR technique of GE. All reconstructed images were standardized to ensure identical image brightness.

3.4. Objective Evaluation of Image Quality

3.4.1. Noise (Primary Outcome)

Several regions of interest (ROIs) were selected from the lung parenchyma, and their standard deviation was measured as the image noise. Lower noise indicated higher image quality. The efficacy of the two algorithms

Table 1. Baseline Clinical Data

Characteristic	MBIR group (n = 51)	ASIR group (n = 51)	t/χ^2	P-value
Age (y)	3.21 ± 2.10	3.07 ± 2.00	0.329	0.743
Gender (boy/girl)	30/21	31/20	0.049	0.825
Body weight (kg)	14.8 ± 3.6	15.1 ± 3.9	0.385	0.701
Disease severity (mild/moderate/severe)	35/14/2	34/15/2	0.073	0.964

Abbreviations: ASIR, adaptive statistical iterative reconstruction; MBIR, model-based iterative reconstruction.

in reducing image noise was assessed by comparing the noise levels of the images reconstructed with the MBIR algorithm and the ASIR algorithm.

3.4.2. Signal to Noise Ratio (Secondary Outcome)

The SNR was calculated as follows: SNR = average CT value of lung parenchyma/noise. A higher SNR indicates a higher ratio of signal to noise in the image, resulting in better image quality. The calculated SNR of the reconstructed images by both algorithms was applied as a measure of their specific performance in improving image quality.

3.4.3. Contras to Noise Ratio (Secondary Outcome)

For the CNR, ROIs were selected from the lung parenchyma and mediastinum to measure corresponding CT values and standard deviations. The CNR was calculated as: CNR = (average CT value of lung parenchyma - average CT value of mediastinum) / mediastinal noise. A higher CNR denotes higher contrast between lung parenchyma and mediastinum, which is beneficial for a clear display of lesions.

3.5. Subjective Evaluation of Image Quality

Two experienced radiologists were responsible for subjective quality scoring on the reconstructed images according to the following criteria:

3.5.1. Image Noise Scoring Criteria (Secondary Outcome)

- 1 point: Noise obviously affecting observation.
- 2 points: Loud noise narrowly allowing observation.
- 3 points: Moderate noise not affecting observation.
- 4 points: Low noise and clear images.
- 5 points: Minimal noise and very clear images.

3.5.2. Microstructure Display (Secondary Outcome)

- 1 point: Almost invisible.
- 2 points: Fuzzy and indistinct.
- 3 points: Partially visible and unclear.
- 4 points: Clear and visible.
- 5 points: Clear, distinct, and rich in detail.

3.5.3. Scoring Criteria for the Definition of Lesion Edges (Secondary Outcome)

- 1 point: Blurry edges with the scope difficult to determine.
- 2 points: Relatively blurry edges with the scope that can be roughly determined.
- 3 points: Clear unsharp edges with the scope that can be generally determined.
- 4 points: Fairly clear boundaries.
- 5 points: Very clear and sharply recognizable edges.

3.5.4. Overall Image Quality (Primary Outcome)

- 1 point: Extremely poor quality, unable to meet diagnostic needs.
- 2 points: Poor quality that can barely be used for diagnosis.
- 3 points: Average quality capable of meeting basic diagnostic needs.
- 4 points: Good quality enabling relatively high accuracy of diagnosis.
- 5 points: Very good quality with high accuracy of diagnosis.

The final result of the subjective quality score was defined as the mean of scores provided by the two radiologists.

3.6. Determination of Radiation Dose

The dose-length product (DLP) and effective dose (ED) (secondary outcomes) of each examination were measured and recorded using the in-built dose monitoring system of the CT equipment. Dose-length product reflected the total radiation dose received by

Table 2. Subjective Quality Evaluation Results of Model-Based Iterative Reconstruction and Adaptive Statistical Iterative Reconstruction Groups

Group	Image noise	Microstructure display	Definition of lesion edges	Overall image quality
MBIR (n = 51)	4.52 ± 0.45	4.72 ± 0.34	4.19 ± 0.37	4.46 ± 0.35
ASIR (n = 51)	3.64 ± 0.57	3.27 ± 0.41	3.33 ± 0.51	3.53 ± 0.50
t	8.653	19.441	9.747	22.582
P-value	0.001	0.001	0.001	0.001

Abbreviations: ASIR, Adaptive statistical iterative reconstruction; MBIR, model-based iterative reconstruction.

the patient during scanning, while ED served as a dose index associated with the risk of radiation-induced carcinogenesis. The effective dose was calculated based on a specific formula, which typically involves multiplying the DLP by a conversion factor that accounts for the sensitivity of the irradiated tissues to radiation.

3.7. Statistical Analysis

Statistical analysis was conducted using SPSS Statistics for Windows, Version 26.0 software (IBM Corp., Armonk, NY, USA). The Kappa test was carried out to analyze the consistency of subjective scores provided by the two radiologists, with the Kappa coefficient and its 95% confidence interval reported. For objective noise values, SNR, and other continuous variables, comparisons between the two groups were performed using the *t*-test. Prior to the *t*-test, the normality of the data was assessed using the Shapiro-Wilk test, and the homogeneity of variances was assessed using Levene's test. Categorical data were compared using the χ^2 test. A P-value of less than 0.05 was considered statistically significant.

4. Results

4.1. Baseline Clinical Data

The baseline characteristics of the two groups were comparable, with no statistically significant differences observed (P > 0.05) (Table 1).

4.2. Subjective Quality Evaluation Results of Model-Based Iterative Reconstruction and Adaptive Statistical Iterative Reconstruction Groups

The two radiologists provided highly consistent subjective evaluation results for the reconstructed images, with a Kappa value of 0.85 (95% confidence interval: 0.80 - 0.90) (Table 2). The images in the MBIR group were superior to those in the ASIR group in terms of image noise, microstructure display, definition of lesion edges, and overall image quality (P < 0.05) (Figure 2).

4.3. Radiation Doses of Model-Based Iterative Reconstruction and Adaptive Statistical Iterative Reconstruction Groups

The DLP and ED decreased in the MBIR group compared with those in the ASIR group (Table 3). Specifically, the MBIR group had a DLP of 98.48 ± 7.63 mGy·cm, while the ASIR group had a DLP of 156.34 ± 18.47 mGy·cm (P = 0.001). Similarly, the ED was significantly reduced in the MBIR group (1.56 ± 0.24 mSv) compared with the ASIR group (2.98 ± 1.25 mSv) (P = 0.001).

4.4. Objective Images of Model-Based Iterative Reconstruction and Adaptive Statistical Iterative Reconstruction Groups

The SNR and CNR of the lung field, main pulmonary artery, and muscle were higher in the MBIR group than in the ASIR group (Table 4). Specifically, the lung field SNR increased by approximately 40%, the main pulmonary artery SNR increased by 82%, and the muscle SNR increased by 112%, with all differences reaching statistical significance (P = 0.001). Similarly, the MBIR algorithm led to a 95% improvement in lung field CNR, a 107% increase in main pulmonary artery CNR, and a 106% rise in muscle CNR (P = 0.001).

5. Discussion

Chest CT scans play a key role in the diagnosis of childhood pneumonia. They provide detailed information about the anatomical structure and lesions in the lungs, assisting doctors in accurately identifying the type, scope, and severity of pneumonia. However, children are particularly sensitive to radiation, and long-term or high-dose radiation exposure may elevate the risk of cancer (9). Therefore, low-dose chest CT scans are significant for diagnosing childhood pneumonia, as

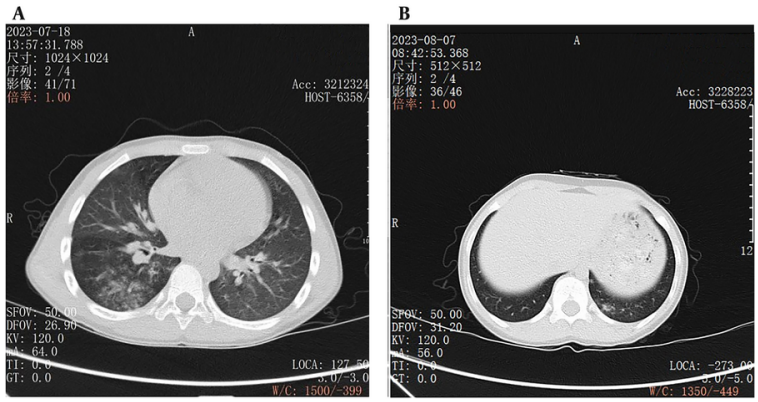

Figure 2. A, An example of a low-dose chest CT image of a child with pneumonia reconstructed by model-based iterative reconstruction (MBIR) algorithm, with the details of the lung structure and lesions clearly displayed; B, An example of a low-dose chest CT image of a pneumonia child reconstructed using adaptive statistical iterative reconstruction (ASIR) algorithm, in which the image noise is lower and the edges of lung markings are more blurred than those in MBIR algorithm.

they reduce the radiation dose while maintaining image quality, thus minimizing potential health hazards (10).

The MBIR algorithm is an advanced image reconstruction technique with several significant advantages. It establishes a precise physical model that considers complex factors such as X-ray transmission, detector response, and photon scattering (11). During reconstruction, MBIR performs multiple iterative computations on raw data to continuously optimize image quality, effectively reducing image noise. Noise in low-dose CT images can affect image definition and readability (12). The MBIR substantially attenuates image noise, increases SNR and CNR, and enhances image definition. It also improves contrast and resolution, particularly in low-dose chest CT images of children with pneumonia. The MBIR can display microstructure features of the lung parenchyma, which are valuable for accurately determining the scope and nature of pneumonia (13). Additionally, MBIR enhances the definition of lesion edges, helping doctors accurately determine lesion scope and morphology, which is crucial for developing effective treatment protocols. Clear lesion edges assist in assessing lesion invasiveness and determining tissue infiltration, providing a reference for selecting therapeutic methods such as surgery, radiotherapy, and chemotherapy (14). High-quality images from MBIR lower the risk of misdiagnosis and missed diagnosis, ensuring timely treatment (15). Accurate determination of pneumonia type is essential for selecting appropriate therapies, and MBIR's high-quality images aid in identifying pneumonia types for individualized treatment protocols.

The ASIR algorithm is a statistical MBIR technique that uses prior knowledge and statistical information for iterative reconstruction, reducing noise and improving image quality (16). However, ASIR is less capable than MBIR in enhancing image quality. In low-dose chest CT images of children with pneumonia, ASIR is inferior to MBIR in microstructure display, lesion edge definition, and overall image quality, though it reduces noise to some extent (16). The ASIR may not display microstructures as clearly as MBIR, potentially affecting accurate judgment of lesion scope and nature. ASIR may also struggle to present lesion edges clearly, complicating the determination of lesion scope and morphology. Overall, ASIR-reconstructed images may be less clear and accurate than MBIR-reconstructed images, influencing diagnostic accuracy.

In this study, two experienced radiologists conducted subjective evaluations of the reconstructed images, showing high consistency and reliability. The evaluations covered image noise, microstructure display, lesion edge definition, and overall image quality. Results indicated that MBIR produced better images than ASIR in all aspects, aligning with objective measurements and confirming MBIR's advantages in optimizing low-dose chest CT image quality for children with pneumonia. Subjective evaluation is vital for clinical diagnosis (17).

Table 3. Radiation Doses of Model-Based Iterative Reconstruction and Adaptive Statistical Iterative Reconstruction Groups

Group	Number	DLP (mGy·cm)	ED (mSv)
MBIR	51	98.48 ± 7.63	1.56 ± 0.24
ASIR	51	156.34 ± 18.47	2.98 ± 1.25
t	-	20.676	7.967
P-value	-	0.001	0.001

Abbreviations: ASIR, adaptive statistical iterative reconstruction; DLP, dose-length product; ED, effective dose; MBIR, model-based iterative reconstruction.

Table 4. Objective Images of Model-Based Iterative Reconstruction and Adaptive Statistical Iterative Reconstruction Groups

Group	SNR			CNR		
	Lung field	Main pulmonary artery	Muscle	Lung field	Main pulmonary artery	Muscle
MBIR (n = 51)	31.32 ± 12.11	5.41 ± 2.26	12.36 ± 2.32	42.98 ± 10.43	18.52 ± 5.23	13.87 ± 2.57
ASIR (n = 51)	22.41 ± 9.82	2.97 ± 1.67	5.84 ± 1.37	22.05 ± 7.36	8.94 ± 2.34	6.74 ± 1.83
t	4.081	6.200	17.281	11.709	11.940	16.139
P-value	0.001	0.001	0.001	0.001	0.001	0.001

Abbreviations: ASIR, Adaptive statistical iterative reconstruction; CNR, contrast-to-noise ratio; MBIR, model-based iterative reconstruction; SNR, signal-to-noise ratio.

Radiologists primarily rely on image observation for diagnosis in their daily work, so image quality directly impacts diagnostic accuracy (18). The MBIR algorithm can reconstruct higher-quality images, providing doctors with more distinct and accurate information. In diagnosing childhood pneumonia, accurate diagnosis is foundational for formulating effective treatment protocols. Inaccurate diagnosis may lead to improper treatment, disease exacerbation, or missed treatment opportunities, potentially resulting in serious consequences for children (19). Therefore, improving image quality is vital for diagnosing and treating childhood pneumonia.

From the perspective of radiation dose, this study found that the MBIR group had lower DLP and ED than the ASIR group, suggesting that the MBIR algorithm also has advantages in decreasing radiation dose. Reducing radiation dose is especially important for child patients in clinical practice. Children in growth and development stages have immature organs and systems, making them more sensitive to radiation. Minimizing potential radiation hazards to children's health is crucial. Although low-dose CT scans reduce radiation dose, further reduction is possible with advanced image reconstruction algorithms like MBIR. This is of great clinical value for children requiring multiple CT scans, as it reduces cumulative radiation dose and lowers cancer risk. The reduction in radiation dose also aligns with medical ethics, reflecting care and protection for patients.

Signal-to-noise ratio and CNR are vital objective indexes of image quality. This study revealed increases in SNR and CNR in the MBIR group compared to the ASIR group, indicating that MBIR-reconstructed images excel in SNR and contrast between lung parenchyma and mediastinum. High SNR and CNR facilitate visualizing lung lesions and enhance diagnostic accuracy. In low-dose chest CT images of children with pneumonia, the MBIR algorithm enhances SNR and CNR, allowing doctors to observe differences between pneumonia lesions and surrounding normal tissues more clearly, aiding in accurate identification of lesion scope, nature, and characteristics (20). Clear contrast between lesions and surrounding tissues helps define lesion boundaries and determine invasiveness. High SNR and CNR assist in identifying lesions with unclear boundaries, avoiding missed diagnoses.

However, this study has limitations. The relatively small sample size might impact the generalizability of the results. Future studies could expand the sample size to further validate MBIR's strengths in optimizing low-dose chest CT image quality for children with pneumonia. An enlarged sample size could better reflect conditions across different age groups and severities, enhancing generalizability and reliability (21). Additionally, confounding factors such as operator experience, differences in CT equipment or settings, and

clinical context were not controlled, which may influence result generalizability. Standardization efforts were made, but these variables could introduce variability. Future multicenter studies with diverse clinical contexts and equipment will help further validate the results.

In conclusion, the MBIR algorithm shows significant advantages in optimizing low-dose chest CT image quality for children with pneumonia, reducing radiation dose while ensuring diagnostic accuracy. These improvements in image quality can lead to more accurate lesion detection, better visualization of subtle abnormalities, and more confident decision-making by clinicians, ultimately contributing to more effective management and treatment of pediatric pneumonia.

Footnotes

Authors' Contribution: Y. Y. designed the study. R. C. and W. W. conceived and supervised the study. J. H. and M. G. performed and analyzed the experiments. S. Z. drafted the paper. The first two authors contributed equally to this study.

Conflict of Interests Statement: The authors declare that there are no conflicts of interest.

Data Availability: The data that support the findings of this study are available from the corresponding author upon reasonable request.

Ethical Approval: The study was approved by the ethics committee of Ninghai First Hospital (No. NHEP2023-0112).

Funding/Support: This study was financially supported by 2024 County-Level Social Development (Health System) Science and Technology Plan Project (No. 202430).

Informed Consent: All patients in the study signed the informed consent form.

References

1. Hoste L, Van Paemel R, Haerynck F. Multisystem inflammatory syndrome in children related to COVID-19: a systematic review. *Eur J Pediatr*. 2021;**180**(7):2019-34. [PubMed ID: 33599835]. [PubMed Central ID: PMC7890544]. https://doi.org/10.1007/s00431-021-03993-5.
2. Heiss R, Tan L, Schmidt S, Regensburger AP, Ewert F, Mammadova D, et al. Pulmonary Dysfunction after Pediatric COVID-19. *Radiology*. 2023;**306**(3). e221250. [PubMed ID: 36125379]. [PubMed Central ID: PMC9513839]. https://doi.org/10.1148/radiol.221250.
3. Guitart C, Bobillo-Perez S, Rodriguez-Fanjul J, Carrasco JL, Brotons P, Lopez-Ramos MG, et al. Lung ultrasound and procalcitonin, improving antibiotic management and avoiding radiation exposure in pediatric critical patients with bacterial pneumonia: a randomized clinical trial. *Eur J Med Res*. 2024;**29**(1):222. [PubMed ID: 38581075]. [PubMed Central ID: PMC10998368]. https://doi.org/10.1186/s40001-024-01712-y.
4. Chandran MO, Pendem S, P SP, Chacko C, P, Kadavigere R. Influence of deep learning image reconstruction algorithm for reducing radiation dose and image noise compared to iterative reconstruction and filtered back projection for head and chest computed tomography examinations: a systematic review. *F1000Res*. 2024;**13**:274. [PubMed ID: 38725640]. [PubMed Central ID: PMC11079581]. https://doi.org/10.12688/f1000research.147345.1.
5. Gomi T, Kijima Y, Kobayashi T, Koibuchi Y. Evaluation of a Generative Adversarial Network to Improve Image Quality and Reduce Radiation-Dose during Digital Breast Tomosynthesis. *Diagnostics (Basel)*. 2022;**12**(2). [PubMed ID: 35204582]. [PubMed Central ID: PMC8871529]. https://doi.org/10.3390/diagnostics12020495.
6. Struyf T, Deeks JJ, Dinnes J, Takwoingi Y, Davenport C, Leeflang MM, et al. Signs and symptoms to determine if a patient presenting in primary care or hospital outpatient settings has COVID-19. *Cochrane Database Syst Rev*. 2022;**5**(5). CD013665. [PubMed ID: 35593186]. [PubMed Central ID: PMC9121352]. https://doi.org/10.1002/14651858.CD013665.pub3.
7. Sun J, Peng Y, Duan X, Yu T, Zhang Q, Liu Y, et al. Image quality in children with low-radiation chest CT using adaptive statistical iterative reconstruction and model-based iterative reconstruction. *PLoS One*. 2014;**9**(5). e96045. [PubMed ID: 24828429]. [PubMed Central ID: PMC4020743]. https://doi.org/10.1371/journal.pone.0096045.
8. Sun J, Yu T, Liu J, Duan X, Hu D, Liu Y, et al. Image quality improvement using model-based iterative reconstruction in low dose chest CT for children with necrotizing pneumonia. *BMC Med Imaging*. 2017;**17**(1):24. [PubMed ID: 28302073]. [PubMed Central ID: PMC5356402]. https://doi.org/10.1186/s12880-017-0177-9.
9. Warren KE, Vezina G, Krailo M, Springer L, Buxton A, Peer CJ, et al. Phase II Randomized Trial of Lenalidomide in Children With Pilocytic Astrocytomas and Optic Pathway Gliomas: A Report From the Children's Oncology Group. *J Clin Oncol*. 2023;**41**(18):3374-83. [PubMed ID: 37126770]. [PubMed Central ID: PMC10414716]. https://doi.org/10.1200/JCO.22.01777.
10. Yoon JH, Park JY, Lee SM, Lee ES, Kim JH, Lee JM. Renal protection CT protocol using low-dose and low-concentration iodine contrast medium in at-risk patients of HCC and with chronic kidney disease: a randomized controlled non-inferiority trial. *Cancer Imaging*. 2023;**23**(1):100. [PubMed ID: 37858212]. [PubMed Central ID: PMC10588122]. https://doi.org/10.1186/s40644-023-00616-0.
11. Major VJ, Jones SA, Razavian N, Bagheri A, Mendoza F, Stadelman J, et al. Evaluating the Effect of a COVID-19 Predictive Model to Facilitate Discharge: A Randomized Controlled Trial. *Appl Clin Inform*. 2022;**13**(3):632-40. [PubMed ID: 35896506]. [PubMed Central ID: PMC9329139]. https://doi.org/10.1055/s-0042-1750416.
12. Sanders JW, Venkatesan AM, Levitt CA, Bathala T, Kudchadker RJ, Tang C. Fully balanced SSFP without an endorectal coil for post-implant QA of MRI-assisted radiosurgery (MARS) of prostate cancer: a prospective study. *Int J Radiat Oncol Biol Phys*. 2021;**109**(2):614-25. [PubMed ID: 35427557]. https://doi.org/10.1016/j.ijrobp.2022.01.021.

13. Storoni S, Treurniet S, Micha D, Celli M, Bugiani M, van den Aardweg JG, et al. Pathophysiology of respiratory failure in patients with osteogenesis imperfecta: a systematic review. *Ann Med*. 2021;**53**(1):1676-87. [PubMed ID: 34569391]. [PubMed Central ID: PMC8477932]. https://doi.org/10.1080/07853890.2021.1980819.
14. Chu M, Wang H, Bian L, Huang J, Wu D, Zhang R, et al. Nebulization Therapy with Umbilical Cord Mesenchymal Stem Cell-Derived Exosomes for COVID-19 Pneumonia. *Stem Cell Rev Rep*. 2022;**18**(6):2152-63. [PubMed ID: 35665467]. [PubMed Central ID: PMC9166932]. https://doi.org/10.1007/s12015-022-10398-w.
15. Zhang X, Chen J, Yu N, Ren Z, Tian Q, Tian X, et al. Reducing contrast medium dose with low photon energy images in renal dual-energy spectral CT angiography and adaptive statistical iterative reconstruction (ASIR). *Br J Radiol*. 2021;**94**(1120):20200974. [PubMed ID: 33684310]. [PubMed Central ID: PMC8010535]. https://doi.org/10.1259/bjr.20200974.
16. Noda Y, Nakamura F, Yasuda N, Miyoshi T, Kawai N, Kawada H, et al. Advantages and disadvantages of single-source dual-energy whole-body CT angiography with 50% reduced iodine dose at 40 keV reconstruction. *Br J Radiol*. 2021;**94**(1121):20201276. [PubMed ID: 33617294]. [PubMed Central ID: PMC8506171]. https://doi.org/10.1259/bjr.20201276.
17. Mahadev A, Hentati F, Miller B, Bao J, Perrin A, Kallogjeri D, et al. Efficacy of Gabapentin For Post-COVID-19 Olfactory Dysfunction: The GRACE Randomized Clinical Trial. *JAMA Otolaryngol Head Neck Surg*. 2023;**149**(12):1111-9. [PubMed ID: 37733356]. [PubMed Central ID: PMC10514889]. https://doi.org/10.1001/jamaoto.2023.2958.
18. Li TT, Zhang B, Fang H, Shi M, Yao WQ, Li Y, et al. Human mesenchymal stem cell therapy in severe COVID-19 patients: 2-year follow-up results of a randomized, double-blind, placebo-controlled trial. *EBioMedicine*. 2023;**92**:104600. [PubMed ID: 37149930]. [PubMed Central ID: PMC10161678]. https://doi.org/10.1016/j.ebiom.2023.104600.
19. Pernica JM, Harman S, Kam AJ, Carciumaru R, Vanniyasingam T, Crawford T, et al. Short-Course Antimicrobial Therapy for Pediatric Community-Acquired Pneumonia: The SAFER Randomized Clinical Trial. *JAMA Pediatr*. 2021;**175**(5):475-82. [PubMed ID: 33683325]. [PubMed Central ID: PMC7941245]. https://doi.org/10.1001/jamapediatrics.2020.6735.
20. Bannerji R, Arnason JE, Advani RH, Brown JR, Allan JN, Ansell SM, et al. Odronextamab, a human CD20xCD3 bispecific antibody in patients with CD20-positive B-cell malignancies (ELM-1): results from the relapsed or refractory non-Hodgkin lymphoma cohort in a single-arm, multicentre, phase 1 trial. *Lancet Haematol*. 2022;**9**(5):e327-39. [PubMed ID: 35366963]. [PubMed Central ID: PMC10681157]. https://doi.org/10.1016/S2352-3026(22)00072-2.
21. Schmidt WA, Dasgupta B, Sloane J, Giannelou A, Xu Y, Unizony SH, et al. A phase 3 randomized, double-blind, placebo-controlled study to evaluate the efficacy and safety of sarilumab in patients with giant cell arteritis. *Arthritis Res Ther*. 2023;**25**(1):199. [PubMed ID: 37840134]. [PubMed Central ID: PMC10577982]. https://doi.org/10.1186/s13075-023-03177-6.